Available online at www.sciencedirect.com
SCIENCE DIRECT®
International Journal of Pharmaceutics 293 (2005) 51–62
international journal of pharmaceutics
www.elsevier.com/locate/ijpharm

Molecular interaction in alginate beads reinforced with sodium starch glycolate or magnesium aluminum silicate, and their physical characteristics

Satit Puttipipatkhachorn [a], Thaned Pongjanyakul [b,*], Aroonsri Priprem [b]

[a] *Department of Manufacturing Pharmacy, Faculty of Pharmacy, Mahidol University, Bangkok 10400, Thailand*
[b] *Department of Pharmaceutical Technology, Faculty of Pharmaceutical Sciences, Khon Kaen University, Khon Kaen 40002, Thailand*

Received 11 October 2004; received in revised form 9 December 2004; accepted 11 December 2004

Abstract

Diclofenac calcium–alginate (DCA) beads were reinforced with different amounts of sodium starch glycolate (SSG) or magnesium aluminum silicate (MAS) and were prepared using ionotropic gelation method. Complex formation of sodium alginate (SA) and SSG or MAS in calcium–alginate beads was revealed using FTIR spectroscopy. Differential scanning calorimetric study indicated that diclofenac sodium (DS) in amorphous form was dispersed in the matrix of DCA beads. The thermal behavior of SSG–DCA and MAS–DCA beads was similar to the control bead. Both additives can improve the entrapment efficiency of DCA beads. The swelling and water uptake of the beads depended on the properties of incorporated additives. The SSG–DCA beads showed a higher water uptake and swelling than MAS–DCA beads. Moreover, the swelling of the beads showed a good correlation with the square root of time. The release kinetic of the beads in pH 6.8 phosphate buffer was swelling controlled mechanism, while that in distilled water followed Higuchi's model. The slower release rate and the longer lag time in pH 6.8 phosphate buffer was obtained from the SSG–DCA and MAS–DCA beads because of complex formation between SA and SSG or MAS. However, SSG in the beads could increase the release of DS from the beads in distilled water because it acted as a channeling agent. In contrast, MAS retarded the release of DS from the beads in distilled water due to the stronger matrix formation.

Keywords: Molecular interaction; Calcium–alginate bead; Magnesium aluminum silicate; Sodium starch glycolate; Diclofenac sodium

1. Introduction

Sodium alginate (SA) is a sodium salt of alginic acid, a naturally occurring non-toxic polysaccharide found

* Corresponding author. Tel.: +66 43 362092; fax: +66 43 202379.
E-mail address: thaned@kku.ac.th (T. Pongjanyakul).

0378-5173/$ – see front matter © 2005 Elsevier B.V. All rights reserved.
doi:10.1016/j.ijpharm.2004.12.006

in brown algae. Alginate has been widely used as food and pharmaceutical additives, such as a tablet disintegrant and gelling agent. It contains two uronic acids, α-L-guluronic and β-D-mannuronic acids, and is composed of homopolymeric blocks and blocks with an alternating sequence (Draget, 2000). Gelation occurs by cross-linking of the uronic acids with divalent cations, such as Ca^{2+}. The primary mechanism of this gelation involves extended chain sequences which adopt a regular two-fold conformation and dimerize with specific chelation of Ca^{2+}, the so-called 'egg-box' structure (Grant et al., 1973). Each Ca^{2+} ion takes part in nine co-ordination link with an oxygen atom, resulting in three-dimensional network of calcium–alginate. This phenomenon has been applied for preparing an alginate bead employed as a drug delivery system. The formation of calcium–alginate beads by ionotropic gelation was achieved by dropping the drug-containing SA dispersion into a calcium chloride bath (Østberg et al., 1994; Sugawara et al., 1994).

Small matrices of calcium–alginate beads have been investigated as a controlled release system for drugs and proteins. The calcium–alginate beads could protect an acid-sensitive drugs from gastric juice, and the drug was consequently released from the beads in the intestine (Hwang et al., 1995; Fernández-Hervás et al., 1998). Thus, drug-loaded alginate beads are suitable for nonsteroidal anti-inflammatory drugs, which caused gastric irritation. Moreover, the alginate beads also exhibited a potential for a pulsatile release system of macromolecular drugs (Kikuchi et al., 1997).

Drug released from calcium–alginate beads depends on the swelling of the beads and the diffusion of the drug in the gel matrix (Sugawara et al., 1994). The release characteristics of entrapped substances could be improved by surface complexation of alginate with chitosan, cationic polysaccharide (Murata et al., 1993a; González-Rodríguez et al., 2002), and incorporation of some water-soluble polymers in the beads, such as chondroitin sulfate (Murata et al., 1996), konjac glucomannan (Wang and He, 2002), and gelatin (Almeida and Almeida, 2004). Furthermore, the addition of chitin, water-insoluble polymer, caused a sustained release of drug from the beads in pH 6.8 dissolution medium. This was because of the formation of a complex between the carboxyl groups of alginate and the amino groups of chitin (Murata et al., 2002).

In the present study, we attempted to reinforce calcium–alginate beads containing diclofenac sodium (DS) as a model drug by incorporating sodium starch glycolate (SSG) and magnesium aluminum silicate (MAS). SSG is a sodium salt of a poly-α-glucopyranose in which some of the hydroxyl groups are in the form of the carboxymethyl ether. Hwang et al. (1995) reported that SSG loaded in ibuprofen calcium–alginate beads could alter the release rate of the drug. However, other characteristics of the beads containing SSG were not reported. MAS is used in oral and topical formulations as a suspending and stabilizing agent. There is no previous report about the effect of MAS on characteristics of calcium–alginate beads. Therefore, we intended to investigate molecular interaction between SA and SSG or MAS in calcium–alginate beads and to study the change in physical properties of diclofenac calcium–alginate (DCA) beads when reinforced with different amounts of SSG or MAS.

2. Materials and methods

2.1. Materials

Diclofenac sodium was a gift from Biogena Ltd. (Limassol, Cyprus). Sodium alginate NF17 and magnesium aluminum silicate (Veegum HV) were purchased from Srichand United Dispensary Co., Ltd. (Bangkok, Thailand). Sodium starch glycolate was obtained from Rama Production Co., Ltd. (Bangkok, Thailand). All other reagents used in this study were of analytical grade and used as received.

2.2. Preparation of the DCA beads

SA (1% w/v) was dispersed in distilled water with agitation, and then DS (1% w/v) was added and completely dissolved with a homogenizer for 5 min. DS-SA dispersion (80 ml) was dropped through a no. 18 needle, from hypodermic syringe into 0.45 M calcium chloride solution (200 ml). The gel beads were cured in this solution for 1 h, then filtered, and rinsed several times with distilled water. The beads were dried at room temperature for 48 h, followed at 45 °C for 12–16 h. In order to prepare the MAS–DCA or SSG–DCA beads, MAS (0.5, 1 and 3% w/v) or SSG (0.5, 1 and 2% w/v)

was incorporated in the DS-SA dispersion and then the preparation was proceeded as described above.

2.3. Viscosity measurement

Viscosity of SA, MAS–SA and SSG–SA dispersions at the concentration used in Section 2.2 was measured using small sample adapter of Brookfield digital rheometer (Model DV-III, Brookfield Engineering Labs., Inc., Stoughton, MA) at $32 \pm 1\,^{\circ}C$. Average and standard deviation of three data of the single point viscosity at a shear rate of $22.4\,s^{-1}$ were reported.

2.4. Fourier transform infrared (FTIR) spectroscopy

FTIR spectra of SA, SSG, MAS and the calcium–alginate beads with and without additives (1% w/v SSG and 1% w/v MAS) were recorded with a FTIR spectrophotometer (Spectrum One, Perkin-Elmer, Norwalk, CT) using KBr disc method. Each sample was gently triturated with KBr powder in a weight ratio of 1:100 and then pressed using a hydrostatic press at a pressure of 10 ton for 5 min. The disc was placed in the sample holder and scanned from 4000 to $450\,cm^{-1}$ at a resolution of $4\,cm^{-1}$.

2.5. Particle size and density determinations

Particle size of the DCA beads was determined using an optical microscope (Nikon, Japan). Two hundreds fifty beads were randomized and their Feret's diameters were measured. Density of the DCA beads was measured with a 25 ml-pycnometer by using 0.1 M HCl and calculated as shown in a previous report (Duncan-Hewitt and Grant, 1986). Each determination was conducted in triplicate.

2.6. Drug content determination

Weighed DCA beads were immersed and dispersed in 100 ml of 0.067 M phosphate buffer at pH 6.8 for 12 h. Then, the solution was filtered, and the DS content was assayed by a UV-spectrophotometer (Shimadzu UV1201, Kyoto, Japan) at wavelength of 260 nm. The ratio of the actual to the theoretical drug contents in the DCA beads was termed as entrapment efficiency (Wang and He, 2002).

2.7. Scanning electron microscopic studies

Surface morphology of the DCA beads was characterized before and after release testing in distilled water. Samples of the dried beads were mounted onto stubs, sputter coated with a gold in a vacuum evaporator, and photographed using a scanning electron microscope (Jeol Model JSM-5800LV, Tokyo, Japan).

2.8. Differential scanning calorimetry (DSC)

DSC thermograms of DS, polymers and DCA beads were recorded using a differential scanning calorimeter (DSC822, Mettler Toledo, Switzerland). Each sample (2–2.5 mg) was accurately weighed into a 40-μl aluminum pan without an aluminum cover. The measurement was performed over 30–350 °C at a heating rate of 10 °C/min.

2.9. In vitro drug release studies

A USP dissolution apparatus I (Hanson Research, Northridge, CA) was used to characterize the release of DS from the DCA beads. The baskets were rotated at 50 rpm and $37.0 \pm 0.5\,^{\circ}C$. The dissolution media used were 0.067 M phosphate buffer at pH 6.8 and distilled water. The amount of the DCA beads added to 750 ml dissolution medium was equivalent to DS 25 mg. Samples (7 ml) were collected and replaced with a fresh medium at various time intervals. The amount of drug released was analyzed spectrophotometrically at 260 nm (Shimadzu UV1201, Japan).

The DS release kinetics from DCA beads in various dissolution media were investigated by fitting the DS release data into zero order and Higuchi's model, which can be expressed using Eq. (1) as followed:

$$Q = kt^n \tag{1}$$

where Q is the percentage of drug released at a given time (t), k is the release rate and n is the diffusion exponent. The n value could be defined as 0.5 and 1, which indicated the Higuchi's and zero order equation,

respectively (Costa and Lobo, 2001). The release rate was estimated by fitting the experimental drug release data into both models and analyzed by linear regression analysis.

2.10. Water uptake determination

Weighed DCA beads were placed in a small basket, soaked in 0.067 M phosphate buffer at pH 6.8 or distilled water and shaken occasionally at room temperature (26 ± 1 °C). After a predetermined time interval, each basket was withdrawn, blotted to remove excess water and immediately weighed on an analytical balance (Remuñán-López and Bodmeier, 1997). The water uptake can be calculated from the following equation:

$$\text{Water uptake}\,(\%) = \left(\frac{W_t - W_0}{W_0}\right) \times 100 \qquad (2)$$

where W_t and W_0 are the wet and initial mass of beads, respectively. Water uptake study of DCA beads in pH 6.8 phosphate buffer was performed for 45 min because the swollen beads were broken and could not be blotted to remove an excess water at the longer time.

2.11. Swelling studies

The diameter of DCA beads were measured using a digital caliper (Mitutoyo Model 500-136, Kawasaki, Japan) and then placed in petri disk containing 20 ml of 0.067 M phosphate buffer at pH 6.8 or distilled water at room temperature (26 ± 1 °C). At predetermined time intervals, the diameter of each bead was determined at two different positions, and swelling (%) of the beads was calculated according to Eq. (3) (Talukdar and Kinget, 1995).

$$\text{Swelling}\,(\%) = \left(\frac{D_t - D_0}{D_0}\right) \times 100 \qquad (3)$$

where D_0 and D_t are the initial diameter of the beads and the diameter of the beads at a given time, respectively.

2.12. Statistical analysis

One-way analysis of variance (ANOVA) with the least significant difference (LSD) test for multiple comparisons (SPSS program for MS Windows, release 10.0) was performed to determine the significant effect of entrapment efficiency, water uptake, swelling, and release parameter of the DCA beads. Difference were considered to be significant at a level of $P < 0.05$.

3. Results and discussion

3.1. Effect of SSG and MAS on viscosity of SA dispersion

Interaction of SA with SSG or MAS in dispersion was studied by examining a change in viscosity of the mixtures. The effect of SSG and MAS on the viscosity of 1.5% (w/v) SA dispersion is shown in Table 1. Incorporation of SSG and MAS into SA dispersion caused a significantly higher viscosity ($P < 0.05$) than SA dispersion alone, although the dispersions of 2% (w/v) SSG and 3% (w/v) MAS possessed a low viscosity of 16.8 ± 1.2 and 13.3 ± 0.6 mPa s, respectively. These results indicated the viscosity synergism of SA with SSG or MAS. The viscosity synergism between SA and SSG was a result of the hydrogen bonding of the hydroxyl groups on the glucose residues in SSG with the carboxyl groups of the ionic SA (Walker and Wells, 1982). MAS had many silanol groups on its surface, which had a hydrogen-bonding potential with carboxyl groups of some substances (Gupta et al., 2003). In addition, a small quantity of divalent cations in MAS dispersion, such as aluminium and calcium ions, may interact with

Table 1
Viscosity of sodium alginate and other dispersions in this study

Component	Viscosity at shear rate of 22.4 s^{-1} (mPa s)
1.5% (w/v) SA	132.3 ± 1.5
+0.5% (w/v) SSG	191.3 ± 1.6
+1.0% (w/v) SSG	338.7 ± 2.1
+2.0% (w/v) SSG	635.7 ± 11.0
+0.5% (w/v) MAS	211.0 ± 1.7
+1.0% (w/v) MAS	227.3 ± 5.5
+3.0% (w/v) MAS	426.0 ± 1.7
2% (w/v) SSG	16.8 ± 1.2
3% (w/v) MAS	13.3 ± 0.6

Data are means ± S.D., $n = 3$.

carboxyl groups of SA (Vauthier et al., 1994). This finding was similar to a previous report that viscosity of anionic polymer dispersion was greatly increased by combination with MAS due to synergistic effect (Ciullo, 1981).

3.2. FTIR study

Molecular interaction of SA and SSG or MAS in calcium–alginate beads was investigated using FTIR spectroscopy. FTIR spectra of SA showed the peaks around 3437, 1615, 1417, and 1031 cm^{-1}, indicating the stretching of O–H, COO^- (asymmetric), COO^- (symmetric), and C–O–C, respectively (Fig. 1a). The cross-linking process with calcium ion caused a remarkable shift to higher wavenumber and a decrease in intensity of COO^- stretching peak (Fig. 1b), indicating an ionic bonding between calcium ion and

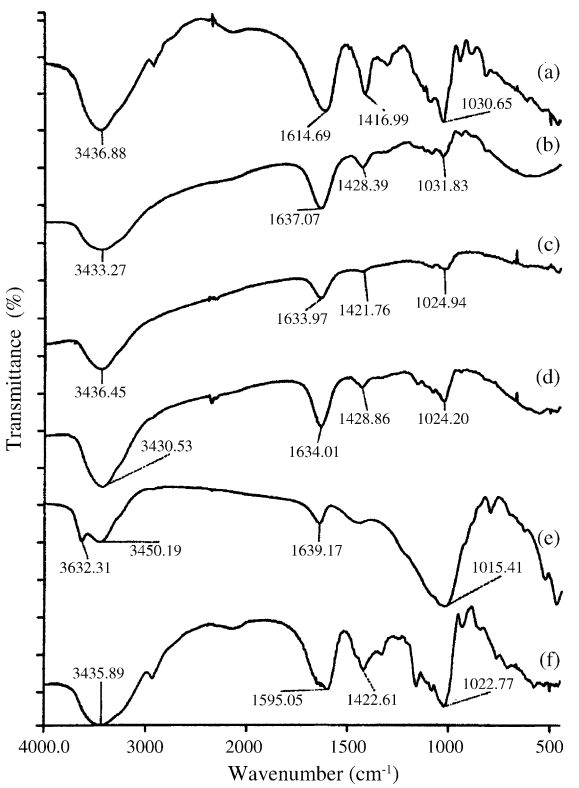

Fig. 1. FTIR spectra of SA (a), calcium–alginate bead (b), calcium–alginate bead prepared using 1% (w/v) MAS (c) and 1% (w/v) SSG (d), MAS (e), and SSG (f).

Table 2
Characteristics of the reinforced DCA beads

Component	Mean diameter[a] (mm)	DS content[b] (% w/w)	EE[b] (%)	pH 6.8 phosphate buffer			Distilled water	
				Release rate[b] (% min^{-1})	Lag time[b] (min)	Swelling rate[c] (% $min^{-1/2}$)	Release rate[b] (% $min^{-1/2}$)	
1.5% (w/v) SA (control)	1.37 ± 0.11	15.9 ± 1.09	39.8 ± 2.73	1.28 ± 0.05 (R^2 = 0.988)	19.4 ± 0.66	21.7 ± 3.57 (R^2 = 0.983)	3.12 ± 0.09 (R^2 = 0.995)	
+0.5% (w/v) SSG	1.58 ± 0.13	15.0 ± 0.09	45.1 ± 0.27	1.02 ± 0.07 (R^2 = 0.999)	23.9 ± 2.86	20.5 ± 0.74 (R^2 = 0.974)	4.55 ± 0.05 (R^2 = 0.994)	
+1.0% (w/v) SSG	1.62 ± 0.16	13.7 ± 0.16	47.9 ± 0.55	1.11 ± 0.09 (R^2 = 0.998)	26.8 ± 1.34	17.1 ± 2.11 (R^2 = 0.978)	5.18 ± 0.02 (R^2 = 0.993)	
+2.0% (w/v) SSG	1.67 ± 0.17	11.8 ± 0.15	52.9 ± 0.67	1.20 ± 0.04 (R^2 = 0.999)	28.2 ± 0.10	15.3 ± 0.71 (R^2 = 0.979)	6.28 ± 0.08 (R^2 = 0.998)	
+0.5% (w/v) MAS	1.52 ± 0.17	14.4 ± 0.27	43.2 ± 0.82	1.36 ± 0.07 (R^2 = 0.986)	28.3 ± 1.20	19.3 ± 3.65 (R^2 = 0.945)	1.88 ± 0.01 (R^2 = 0.998)	
+1.0% (w/v) MAS	1.63 ± 0.23	12.6 ± 0.10	44.0 ± 0.36	1.08 ± 0.06 (R^2 = 0.987)	23.7 ± 1.94	18.7 ± 2.66 (R^2 = 0.989)	1.93 ± 0.08 (R^2 = 0.998)	
+3.0% (w/v) MAS	1.98 ± 0.27	10.3 ± 0.44	56.5 ± 2.40	0.64 ± 0.01 (R^2 = 0.993)	18.9 ± 2.10	15.1 ± 2.28 (R^2 = 0.971)	1.61 ± 0.01 (R^2 = 0.999)	

EE: entrapment efficiency. R^2: determination coefficient.
[a] Data are mean ± S.D., n = 250.
[b] Data are mean ± S.D., n = 3.
[c] Data are mean ± S.D., n = 5.

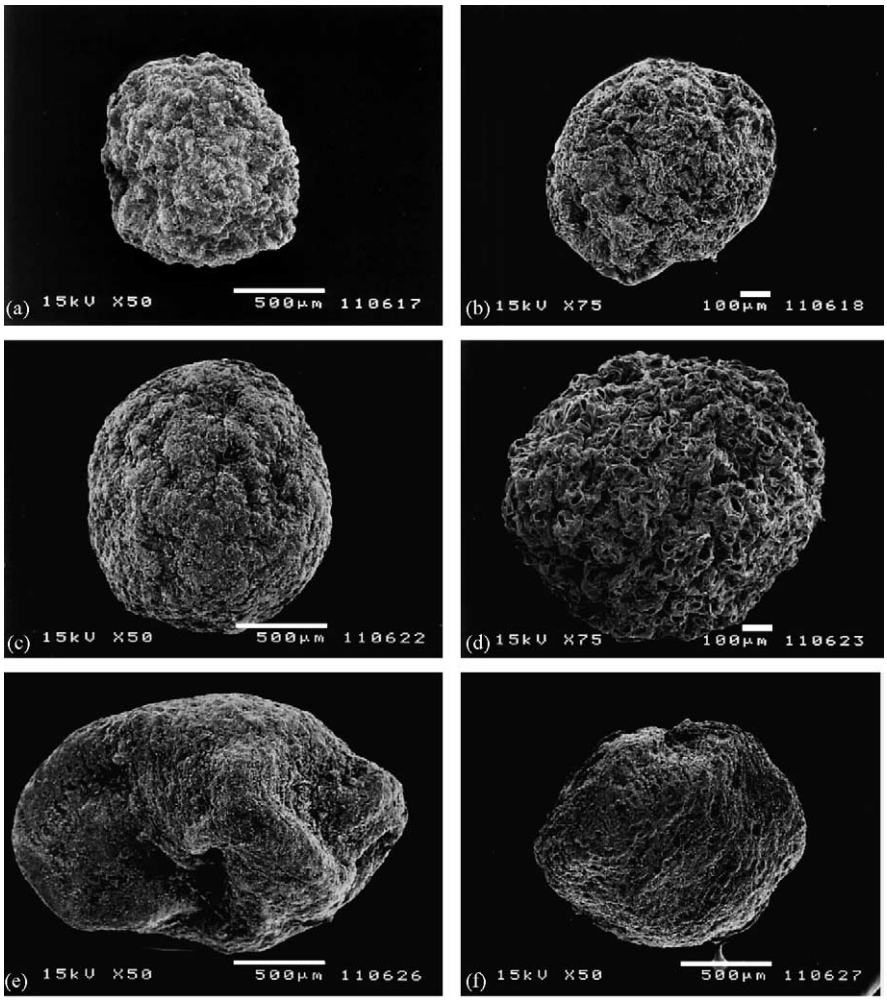

Fig. 2. SEM photographs of control bead, DCA bead prepared by using 2% (w/v) SSG and 3% (w/v) MAS before (a, c, e) and after (b, d, f) release testing in distilled water.

carboxyl groups of SA (Sartori et al., 1997). Moreover, peak at 1031 cm^{-1} of SA showed a decrease in intensity, corresponding to a partial covalent bonding between calcium and oxygen atom (Sartori et al., 1997). Incorporation of MAS into the calcium–alginate beads obviously provided a lower intensity of COO^- stretching peak at 1634 and 1422 cm^{-1} (Fig. 1c) and the O–H stretching peak of SiOH group at 3632 cm^{-1} of MAS disappeared (Fig. 1e). This suggested that silanol groups on the surface of MAS and some divalent ions in MAS could interact with carboxyl groups of SA prior to the cross-linking process and the molecular structure of MAS in the beads might be changed. Similar to MAS, addition of SSG caused a change in FTIR spectra of the calcium–alginate beads (Fig. 1d). The FTIR spectra of the calcium–alginate beads with SSG had a greater intensity and a narrower peak of O–H stretching at 3431 cm^{-1}, indicating a stronger formation of intermolecular hydrogen bonding (Nakanishi and Solomon, 1977), which could confirm the viscosity synergism between SA and SSG. The results indicated that complex formation between SA and SSG or MAS occurred in the dispersion prior to the calcium cross-linking process.

These led to a change in matrix formation of the beads, which could affect the characteristics of DCA beads.

3.3. Physical properties of the reinforced DCA beads

The physical characteristics of the reinforced DCA beads are shown in Table 2. The mean diameters of the SSG–DCA and MAS–DCA beads were obviously greater than those of the control beads. The density of all DCA beads was in the range of 1.67–1.75 g/cm^2. All beads produced were spherical as shown in SEM photographs (Fig. 2a and c), except the MAS–DCA beads were of oval shape with collapsed center (Fig. 2e). The entrapment efficiency of the SSG–DCA and MAS–DCA beads was significantly increased ($P < 0.05$) when compared with the control beads (Table 2). It was indicated that the addition of water-soluble polymers and clay, which interacted with SA caused the increase in barrier for preventing a water leakage from the beads during the preparation period (Dashevsky, 1998). Moreover, the greater bead size provided a higher diffusion pathlength of the drug from the beads. These led to reduce the drug loss from the beads.

3.4. Thermal behavior of the reinforced DCA beads

The DSC thermogram of DS showed an endothermic peak at 55 °C (Fig. 3a). This was due to the evaporation of the water of crystallization (Palomo et al., 1999). The sharp exothermic peak of DS at 280 °C and a small endothermic peak at 284 °C indicated an oxidation reaction between DS and oxygen in air environment and a melting of the compound, respectively (Tudja et al., 2001). SSG and SA showed decomposition peak at 290 and 250 °C, respectively, whereas no decomposition peak of MAS was observed (Fig. 3b–d). The blank beads presented a broad endothermic peak at 70 °C and the exothermic peak of SA was absent (Fig. 3e), indicating the interaction of SA and calcium ion (Fernández-Hervás et al., 1998). This was similar to a DSC thermogram of the control beads (Fig. 3f). These results are in agreement with previous reports (Fernández-Hervás et al., 1998; González-Rodríguez et al., 2002). Benoit et al. (1986) suggested that the lack of endotherms of crystalline drug was observed when drug was molecularly dispersed throughout the polymer. It might lead to conclude that DS in amorphous form was dispersed in the calcium–alginate matrix. The DSC thermograms of the DCA beads prepared using

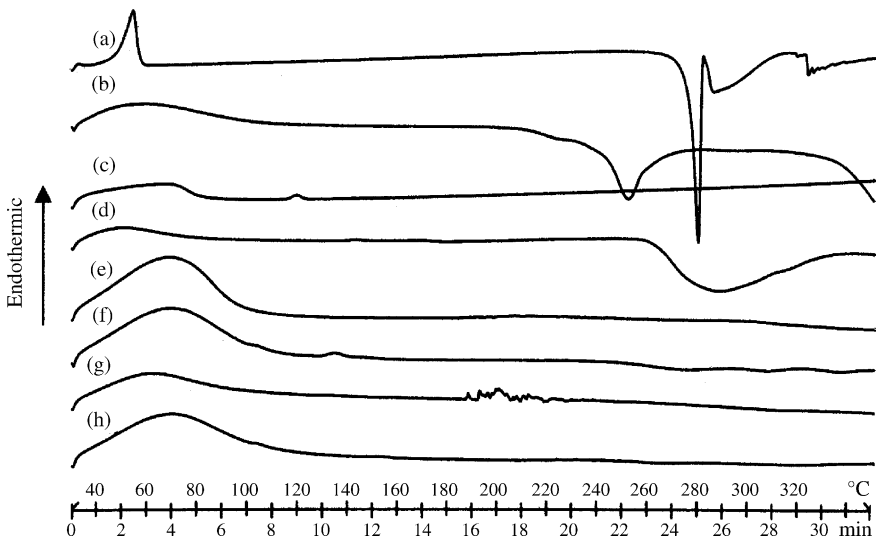

Fig. 3. DSC thermograms of DS (a), SA (b), MAS (c), SSG (d), calcium–alginate bead (e), control bead (f), and DCA bead prepared using 2% (w/v) SSG (g) and 3% (w/v) MAS (h).

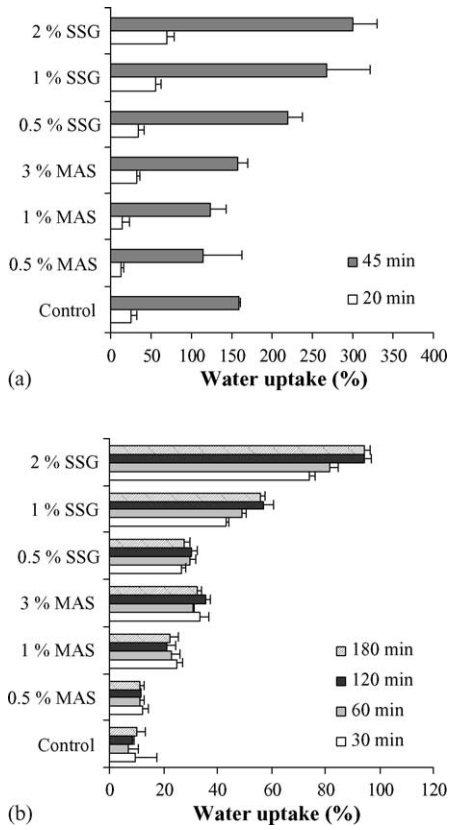

Fig. 4. Water uptake of DCA beads containing different amounts of SSG and MAS in pH 6.8 phosphate buffer (a) and distilled water (b). Each value is the mean ± S.D., $n = 3$.

2% (w/v) SSG (Fig. 3g) and 3% (w/v) MAS (Fig. 3h) were also similar to that of the control beads (Fig. 3f). This suggested that incorporation of SSG and MAS did not affect the thermal property of the DCA beads.

3.5. Water uptake and swelling of the reinforced DCA beads

The water uptake of the reinforced DCA beads in pH 6.8 phosphate buffer is shown in Fig. 4a. The percent water uptake of the SSG–DCA beads in pH 6.8 phosphate buffer at 20 and 45 min was significantly higher ($P < 0.05$) than that of the control bead. On the other hand, the DCA beads prepared from 0.5 and 1% (w/v) MAS gave a significantly lower water uptake at 20 min ($P < 0.05$), whereas the percent water uptake at 45 min was not statistical difference when compared to the control beads. The percent water uptake in distilled water was significantly lower ($P < 0.05$) than that in pH 6.8 phosphate buffer (Fig. 4b). The equilibrium time of water uptake of the MAS–DCA and SSG–DCA beads was 30 and 120 min, respectively. It was found that the higher the content of MAS or SSG, the greater the water uptake of the DCA beads in this medium. Moreover, incorporation of SSG caused a higher water uptake efficiency of the DCA beads than MAS.

Apart from the water uptake study, the swelling profiles of the reinforced DCA beads in pH 6.8 phosphate buffer and distilled water are shown in Fig. 5. The swelling equilibrium time in pH 6.8 phosphate buffer of the beads was approximately 120 min (Fig. 5a and b). It was observed that the higher the amount of SSG and MAS in the beads, the lower the percent swelling at equilibrium. The percent swelling of the DCA beads in pH 6.8 phosphate buffer showed a good correlation with the square root of time ($R^2 > 0.95$) when analyzed by linear regression analysis (Table 2). The swelling rate of the beads prepared using 2% (w/v) SSG or 3% (w/v) MAS was statistically lower ($P < 0.05$) than that of the control beads. In distilled water, the swelling rate of the beads cannot be estimated because of the lower swelling of the beads in this medium. The percent swelling of the beads increased with increasing amount of SSG, but not observed with the beads containing MAS (Fig. 5c and d).

The water uptake and swelling of the beads in pH 6.8 phosphate buffer was higher than those in distilled water because calcium ions cross-linked with alginate were rapidly exchanged with sodium ions in phosphate buffer (Østberg et al., 1994). The partial formation of SA induced water uptake into the beads. Moreover, calcium–alginate gels could be solubilized by the addition of phosphate ion, which acted as calcium ions complexing agent at a pH above 5.5 (Remuñán-López and Bodmeier, 1997). The incorporation of SSG caused a greater water uptake of the DCA beads than MAS because SSG showed the higher rate and amount of water uptake when compared to other superdisintegrants (Visavarungroj and Remon, 1990). In addition, it has been reported that the water uptake of tablets containing SSG was higher than that containing silicon dioxide, the main component of MAS (Wan and Prasad, 1998). However, incorporation of SSG and MAS into the beads led to increasing of the water uptake, but decreasing of the swelling rate in pH 6.8 phosphate buffer. This was due to the results of complexation

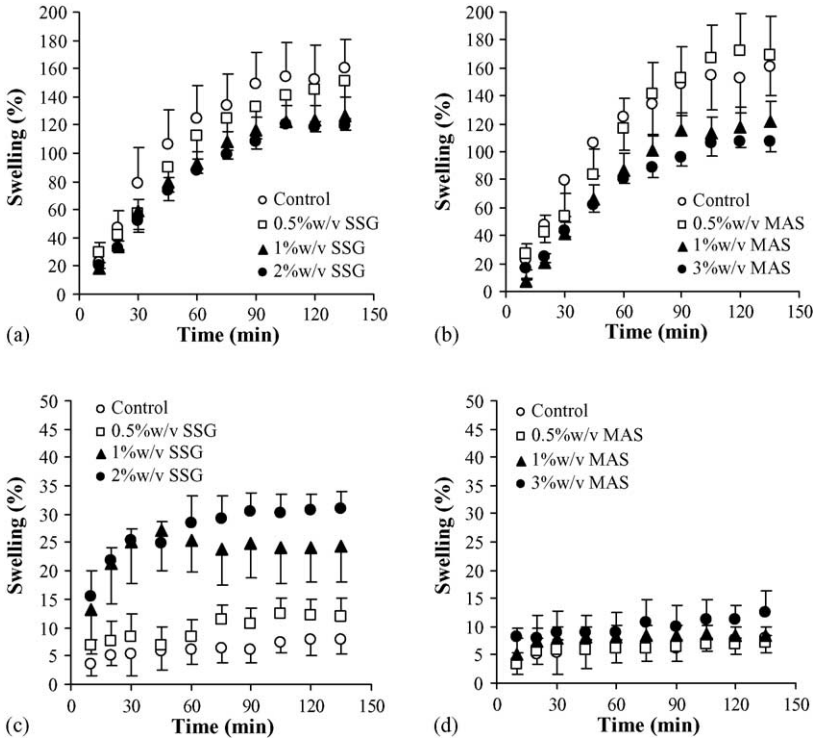

Fig. 5. Swelling profiles of DCA beads containing different amounts of SSG and MAS in pH 6.8 phosphate buffer (a, b) and distilled water (c, d). Each point is the mean ± S.D., $n = 5$.

between alginate and SSG or MAS, which could stabilize the dimension of the beads at the initial period of swelling. The effect of SSG and MAS on water uptake and swelling was clearly demonstrated in distilled water because calcium–alginate beads existed as a stable polymer matrix. The increase in water uptake and swelling of the beads depended on the amount and the properties of the additive substances.

The swelling behavior of the DCA beads in pH 6.8 phosphate buffer was similar to that of hydrophilic polymer tablets. Lee and Peppas (1987) found that the thickness of the gel layer in the tablets increased as a function of the square root of time. Furthermore, the axial and radial swelling rate of xanthan gum tablets could be calculated from the slope of the relationship between the percent swelling and square root of time (Talukdar and Kinget, 1995). However, the difference in swelling between the calcium–alginate beads and the hydrophilic polymer tablets was the occurrence of the ion exchange process before the hydration of polymer molecules on the surface of the beads.

3.6. In vitro release of the reinforced DCA beads

The release profiles of DS from the reinforced DCA beads in pH 6.8 phosphate buffer and distilled water are shown in Fig. 6. The release profile of DS in pH 6.8 phosphate buffer showed a sigmoidal profile with a complete release (Fig. 6a and b). A lag time and a good fitting into zero order kinetic with $R^2 > 0.98$ were found in the DS released not more than 70%. This indicated swelling controlled mechanism. The lag time of the beads containing SSG (0.5–2.0% w/v) and MAS (0.5–1.0% w/v) was statistically longer ($P < 0.05$) than that of the control bead (Table 2). The release rate of the SSG–DCA and MAS–DCA beads was obviously lower than that of the control beads. Particularly, the beads prepared using 3% (w/v) MAS showed the slowest release of DS. However, the disintegration of the swollen beads was observed around 75–90 min of the test. In distilled water, incomplete release of DS for 8 h was obtained (Fig. 6c and d). The release of DS in distilled water did not show the lag time and can

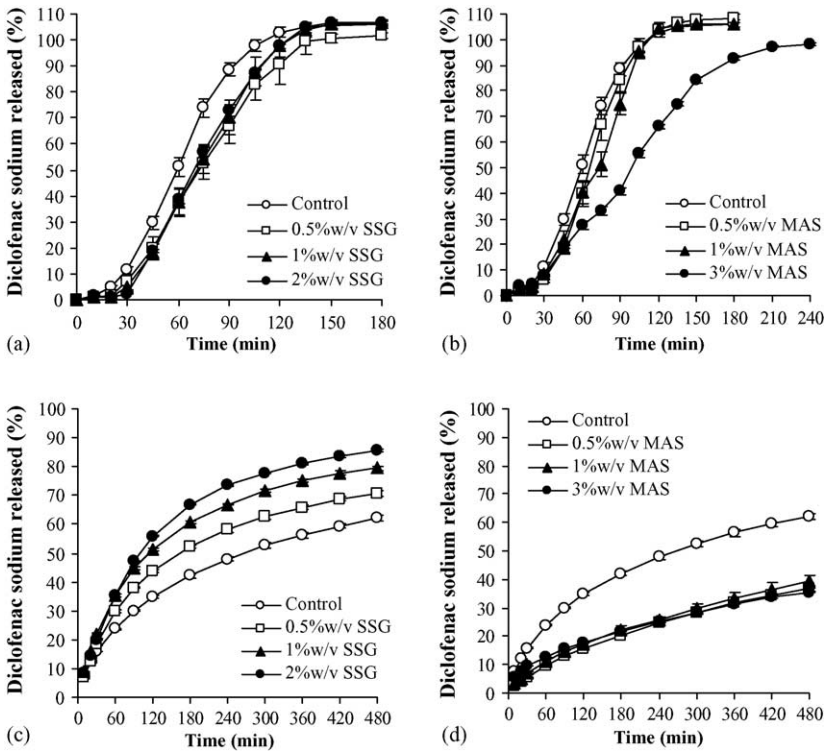

Fig. 6. Release profiles of DCA beads containing different amounts of SSG and MAS in pH 6.8 phosphate buffer (a, b) and distilled water (c, d). Each point is the mean ± S.D., $n = 3$.

be described using Higuchi's model. The release rate of DS from the SSG–DCA beads was significantly increased ($P < 0.05$) with increasing the amount of SSG in the beads. On the other hand, MAS loaded in the beads retarded the release rate of DS, which was not correlated with the amount of MAS in the beads. The DS released at 8 h of the SSG–DCA beads increased with increasing in the water uptake at equilibrium of the beads (Fig. 7a). On the other hand, amount of DS released from the MAS–DCA beads at 8 h was lower than that from the control beads and was fairly constant with increasing amount of MAS, although the water uptake was increased (Fig. 7b). SEM photographs of the beads after release testing in distilled water showed the erosion of the surface of the control bead (Fig. 2b), many small pores of the SSG–DCA bead (Fig. 2d), and no pore formation of the MAS–DCA bead (Fig. 2f). Moreover, it could be observed from SEM studies that the bead sizes after release testing were smaller than that before release testing, indicating the release of alginate (Murata et al., 1993b) and the additive substances incorporated in the beads.

The release of DS from the beads in pH 6.8 phosphate buffer was depressed by the formation of the gel layer at the initial stage but gradually enhanced by the increasing water content and the erosion of the swollen gel phase at the later stage (Sugawara et al., 1994). This can be described by using the ion exchange between calcium ion in the beads and sodium ion in the medium (Kikuchi et al., 1997). In the first stage, calcium ions interacting with carboxylic group in alginate, but not taking part in the egg-box formation, are preferentially released through ion exchange with sodium ion in the medium. Almost negligible alginate disintegration at this stage was probably due to the relatively stable association of calcium ions with polyguluronate sequences, which served as stable cross-linking points within the gels. Alginate disintegration occurred when the calcium ion in the egg-box structure started to release for exchange with sodium ion. Moreover, the lag

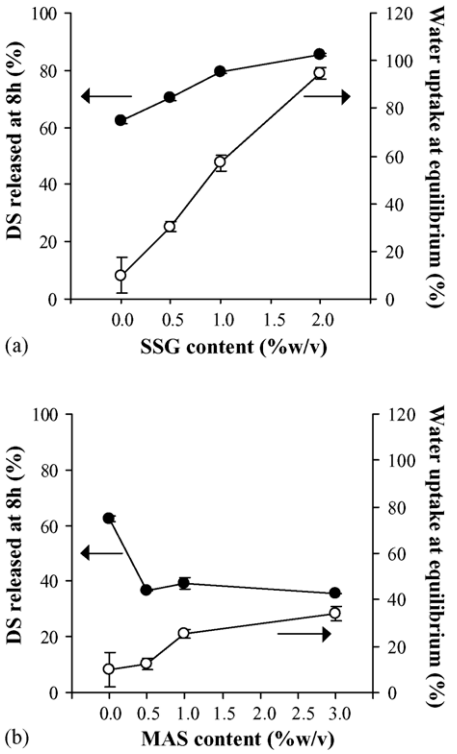

Fig. 7. Relationship between amount of diclofenac sodium released at 8 h and water uptake at equilibrium of DCA beads containing different amounts of SSG (a) and MAS (b) in distilled water. Each point is the mean ± S.D., $n = 3$.

time of release profile occurred because the solubility of DS was decreased with the presence of sodium ions. This was due to the common ion effect (Sheu et al., 1992). The lower release rate and longer lag time of the SSG–DCA and MAS–DCA beads was observed. This can be explained using the complexation of SA and SSG or MAS, which led to increase in tortuosity of the swollen beads. Additionally, this caused the stronger gel matrix and the slower disintegration of the beads, which led to the slower release rate of DS from the beads prepared using 3% (w/v) MAS.

The release of DS from DCA beads in distilled water was slower than that in pH 6.8 phosphate buffer because the DCA beads was stable with the small amount of calcium released (Østberg et al., 1994). Thus, the release mechanism of DS from the beads was matrix diffusion-controlled. The faster release of DS from the SSG–DCA beads was found because of the higher water uptake and the release of free SSG from the beads, which created a channel for drug release. In contrast with SSG, the release of DS was retarded with incorporation of MAS in the beads, which was due to restricted entry of water and dense structure of the matrix.

4. Conclusions

Molecular interaction of SA with SSG or MAS caused a change of characteristics of DCA beads. The beads containing either SSG or MAS provided the higher entrapment efficiency of DS. The swelling and water uptake of the beads depended on the properties of additives. SSG–DCA beads showed a higher water uptake and swelling than MAS–DCA beads. Moreover, the release rate of DS from SSG–DCA and MAS–DCA beads in pH 6.8 phosphate buffer was obviously lower than that from the control beads because of a higher tortuosity in the swollen gel beads, which resulted from the complexation between SA and SSG or MAS. This study also found that SSG in the beads acted as a channeling agent and made the faster release rate of DS in distilled water, whereas MAS in the beads retarded the drug release.

Acknowledgements

The authors wish to thank P. Sri-udon and S. Kanjanabat for laboratory assistance and Faculty of Pharmaceutical Sciences, Khon Kaen University, Khon Kaen, Thailand, and Faculty of Pharmacy, Mahidol University, Bangkok, Thailand for technical supports.

References

Almeida, P.F., Almeida, A.J., 2004. Cross-linked alginate-gelatin beads: a new matrix for controlled release of pindolol. J. Control. Release 97, 431–439.

Benoit, J.P., Courteille, F., Thies, C., 1986. A physicochemical study of the morphology of progesterone loaded poly(D,L-lactide) microspheres. Int. J. Pharm. 29, 95–102.

Ciullo, P.A., 1981. Rheological properties of magnesium aluminum silicate/xanthan gum dispersions. J. Soc. Cosmet. Chem. 32, 275–285.

Costa, P., Lobo, J.M.S., 2001. Modeling and comparison of dissolution profiles. Eur. J. Pharm. Sci. 13, 123–133.

Dashevsky, A., 1998. Protein loss by the microencapsulation of an enzyme (lactase) in alginate beads. Int. J. Pharm. 161, 1–5.

Draget, K.I., 2000. Alginates. In: Philips, G.O., Williams, P.A. (Eds.), Handbook of Hydrocolloids. Woodhead Publishing, Cambridge, pp. 379–395.

Duncan-Hewitt, W.C., Grant, D.J.W., 1986. True density and thermal expansivity of pharmaceutical solids: comparison of methods and assessment of crystallinity. Int. J. Pharm. 28, 75–84.

Fernández-Hervás, M.J., Holgado, M.A., Fini, A., Fell, J.T., 1998. In vitro evaluation of alginate beads of a diclofenac salt. Int. J. Pharm. 163, 23–34.

Grant, G.T., Morris, E.R., Rees, D.A., Smith, P.J.C., Thom, D., 1973. Biological interaction between polysaccharides and divalent cation: the egg-box model. FEBS Lett. 32, 195–198.

González-Rodríguez, M.L., Holgado, M.A., Sánchez-Lafuente, C., Rabasco, A.M., Fini, A., 2002. Alginate/chitosan particulate systems for sodium diclofenac release. Int. J. Pharm. 232, 225–234.

Gupta, M.K., Vanwert, A., Bogner, R.H., 2003. Formation of physical stable amorphous drugs by milling with Neusilin. J. Pharm. Sci. 92, 536–551.

Hwang, S.J., Rhee, G.J., Lee, K.M., Oh, K.H., Kim, C.K., 1995. Release characteristics of ibuprofen from excipient-loaded alginate gel beads. Int. J. Pharm. 116, 125–128.

Kikuchi, A., Kawabuchi, M., Sugihara, M., Sakurai, Y., Okano, T., 1997. Pulsed dextran release from calcium–alginate gel beads. J. Control. Release 47, 21–29.

Lee, P.I., Peppas, N.A., 1987. Prediction of polymer dissolution in swellable controlled-release systems. J. Control. Release 6, 207–215.

Murata, Y., Maeda, T., Miyamoto, E., Kawashima, S., 1993a. Preparation of chitosan-reinforced alginate gel beads-effects of chitosan on gel matrix erosion. Int. J. Pharm. 96, 139–145.

Murata, Y., Miyamoto, E., Kawashima, S., 1996. Additive effect of chondroitin sulfate and chitosan on drug release from calcium-induced alginate gel beads. J. Control. Release 38, 101–108.

Murata, Y., Nakada, K., Miyamoto, E., Kawashima, S., Seo, S.H., 1993b. Influence of erosion of calcium-induced alginate gel matrix on the release of brilliant blue. J. Control. Release 23, 21–26.

Murata, Y., Tsumoto, K., Kofuji, K., Kawashima, S., 2002. Effect of natural polysaccharide addition on drug release from calcium-induced alginate gel beads. Chem. Pharm. Bull. 51, 218–220.

Nakanishi, K., Solomon, P.H., 1977. Infrared Absorption Spectroscopy, second ed. Holden-Day, Inc., San Francisco, pp. 25–30.

Østberg, T., Lund, E.M., Graffner, C., 1994. Calcium–alginate matrices for oral multiple unit administration: IV release characteristics in different media. Int. J. Pharm. 112, 241–248.

Palomo, M.E., Ballesteros, M.P., Frutos, P., 1999. Analysis of diclofenac sodium and derivatives. J. Pharm. Biomed. Anal. 21, 83–94.

Remuñán-López, C., Bodmeier, R., 1997. Mechanical, water uptake and permeability properties of crosslinked chitosan glutamate and alginate films. J. Control. Release 44, 215–225.

Sartori, C., Finch, D.S., Ralph, B., 1997. Determination of the cation content of alginate thin films by FTIR spectroscopy. Polymer 38, 43–51.

Sheu, M.T., Chou, H.L., Kao, C.C., Liu, C.H., Sokoloski, T.D., 1992. Dissolution of diclofenac sodium from matrix tablets. Int. J. Pharm. 85, 57–63.

Sugawara, S., Imai, T., Otagiri, M., 1994. The controlled release of prednisolone using alginate gel. Pharm. Res. 11, 272–277.

Talukdar, M.M., Kinget, R., 1995. Swelling and drug release behaviour of xanthan gum tablets. Int. J. Pharm. 120, 63–72.

Tudja, P., Khan, M.Z.I., Meštrović, E., Horvat, M., Golja, P., 2001. Thermal behaviour of diclofenac sodium: decomposition and melting characteristics. Chem. Pharm. Bull. 49, 1245–1250.

Vauthier, C., Rajaonarivony, M., Couarraze, G., Couvreur, P., Puisieux, F., 1994. Characterization of alginate pregel by rheological investigation. Eur. J. Pharm. Biopharm. 40, 218–222.

Visavarungroj, N., Remon, J.P., 1990. Crosslinked starch as a disintegrating agent. Int. J. Pharm. 62, 125–131.

Walker, C.V., Wells, J.I., 1982. Rheological synergism between ionic and non-ionic cellulose gums. Int. J. Pharm. 11, 309–322.

Wan, L.S.C., Prasad, K.P.P., 1998. Uptake of water by excipients in tablets. Int. J. Pharm. 50, 147–153.

Wang, K., He, Z., 2002. Alginate-konjac glucomannan-chitosan beads as controlled release matrix. Int. J. Pharm. 244, 117–126.